Spectral method for the correction of the Cerenkov light effect in plastic scintillation detectors: A comparison study of calibration procedures and validation in Cerenkov light-dominated situations

Mathieu Guillot, Luc Gingras, and Louis Archambault
Département de Physique, de Génie Physique et d'Optique, Université Laval, Québec, Québec G1K 7P4, Canada and Département de Radio-Oncologie, Hôtel-Dieu de Québec, Centre Hospitalier Universitaire de Québec, Québec, Québec G1R 2J6, Canada

Sam Beddar[a)]
Department of Radiation Physics, Unit 94, The University of Texas M. D. Anderson Cancer Center, 1515 Holcombe Blvd., Houston, Texas 77030

Luc Beaulieu
Département de Physique, de Génie Physique et d'Optique, Université Laval, Québec, Québec G1K 7P4, Canada and Département de Radio-Oncologie, Hôtel-Dieu de Québec, Centre Hospitalier Universitaire de Québec, Québec, Québec G1R 2J6, Canada

(Received 11 August 2010; revised 13 January 2011; accepted for publication 15 February 2011; published 24 March 2011)

Purpose: The purposes of this work were: (1) To determine if a spectral method can accurately correct the Cerenkov light effect in plastic scintillation detectors (PSDs) for situations where the Cerenkov light is dominant over the scintillation light and (2) to develop a procedural guideline for accurately determining the calibration factors of PSDs.
Methods: The authors demonstrate, by using the equations of the spectral method, that the condition for accurately correcting the effect of Cerenkov light is that the ratio of the two calibration factors must be equal to the ratio of the Cerenkov light measured within the two different spectral regions used for analysis. Based on this proof, the authors propose two new procedures to determine the calibration factors of PSDs, which were designed to respect this condition. A PSD that consists of a cylindrical polystyrene scintillating fiber (1.6 mm^3) coupled to a plastic optical fiber was calibrated by using these new procedures and the two reference procedures described in the literature. To validate the extracted calibration factors, relative dose profiles and output factors for a 6 MV photon beam from a medical linac were measured with the PSD and an ionization chamber. Emphasis was placed on situations where the Cerenkov light is dominant over the scintillation light and on situations dissimilar to the calibration conditions.
Results: The authors found that the accuracy of the spectral method depends on the procedure used to determine the calibration factors of the PSD and on the attenuation properties of the optical fiber used. The results from the relative dose profile measurements showed that the spectral method can correct the Cerenkov light effect with an accuracy level of 1%. The results obtained also indicate that PSDs measure output factors that are lower than those measured with ionization chambers for square field sizes larger than 25×25 cm^2, in general agreement with previously published Monte Carlo results.
Conclusions: The authors conclude that the spectral method can be used to accurately correct the Cerenkov light effect in PSDs. The authors confirmed the importance of maximizing the difference of Cerenkov light production between calibration measurements. The authors also found that the attenuation of the optical fiber, which is assumed to be constant in the original formulation of the spectral method, may cause a variation of the calibration factors in some experimental setups. [DOI: 10.1118/1.3562896]

Key words: plastic scintillation detectors, Cerenkov radiation, radiation detectors, calibration, dosimetry

I. INTRODUCTION

The reliability and efficacy of radiation treatments depend strongly on the accuracy of dose measurements performed during the initial commissioning of the treatment system and during the verification of treatment plans. Over the years, research resources have been devoted to the development and characterization of radiation detectors with the aim to continuously improve the accuracy of dose measurements. In spite of these efforts, radiation detectors still have limitations when used in the context of advanced treatment modalities, such as intensity-modulated radiation therapy and radiosurgery, due to the small field sizes, steep dose gradi-

ents, beam incidence angle variations, and nonequilibrium charge particle conditions.[1] These limitations are usually overcome by applying correction factors to the detector response.

Plastic scintillation detectors (PSDs) have been previously used to perform photon, electron, and proton beam dosimetry.[2–5] PSDs use plastic scintillators to convert the energy absorbed in a medium at the scintillator's location into visible light that can be read using a photodetector. Two types of plastic scintillators are commonly used for radiation detection: (1) Polymer scintillators, in which scintillating organic molecules are dissolved in a polyvinyl toluene solvent, and (2) scintillating fibers, which are polystyrene core optical fibers doped with scintillating organic molecules and surrounded by a polymethyl methacrylate (PMMA) cladding. Optical fibers or bulky transparent materials can be used to transport the scintillation light to the photodetector. One major advantage of PSDs is that they can be made entirely from nearly water-equivalent plastic materials.[2,6] Many units can therefore be stacked in an array without perturbing the delivered dose distribution. PSDs are characterized by a unique set of properties including high spatial resolution, angular independence, energy independence to megavoltage energy photon and electron beams, dose rate independence, real-time readout, and high sensitivity, which makes them suitable for measuring complex dose distributions.[2,7,8]

One important factor that influences the accuracy of PSDs is the production, in the optical light guide, of a contamination signal called Cerenkov light, which is added to the scintillation signal and which prevent the direct measurement of the scintillation light intensity.[9] The Cerenkov light is produced in any dielectric medium when charged particles are traveling faster than the speed of light in that medium.[10] The emission spectrum covers the entire visible domain and the threshold energy of production depends on the refractive index of the medium and the type of charged particles (for electrons, this threshold energy is 178 keV in PMMA and 144 keV in polystyrene). Beddar *et al.*[7,11] proposed the first method to correct for the effect of Cerenkov light in PSDs. They used a device made of two parallel adjacent optical fibers in which only one optical fiber was coupled to a scintillator. Because the signal of the uncoupled optical fiber is composed only of Cerenkov light, the signal difference between the two optical fibers can be attributed to the scintillation intensity in the PSD. Although this method is accurate in most situations, it has been shown to yield inaccurate results in steep dose gradient conditions because the Cerenkov light can be generated with different intensities in the adjacent optical fibers.[12] Lambert *et al.*[13,14] introduced an alternative approach to address the issue of Cerenkov light. They developed a Cerenkov-free PSD by coupling a plastic scintillator to an air core light guide made from a hollow silica tube coated inside with a thin layer of silver. No Cerenkov light is produced in air because the refractive index of air is close to unity. However, this method uses non-water-equivalent materials that can perturb the delivered dose distribution, especially if multiple units are stacked. Lambert *et al.*[14] reported depth-dose measurements that agreed with ionization chamber measurements to within 1.6% for photon beams but with discrepancies of up to 4.5% for electron beams. These results are not as accurate as those obtained with PSDs made entirely from nearly water-equivalent plastic materials, which have been shown to agree with ionization chambers to within 2% for photon beams from cobalt-60 to 25 MV and electron beams from 6 to 21 MeV.[3,7] Recently, Lacroix *et al.*[15] used a PSD as a perturbation-free reference detector to experimentally extract the product of the wall and replacement correction factors ($P_{\mathrm{Wall}} \cdot P_{\mathrm{Repl.}}$) for two parallel-plate ionization chambers in 6, 12, and 18 MeV electron beams. Their results were in close agreement with those of Monte Carlo simulations in water medium performed by other investigators.

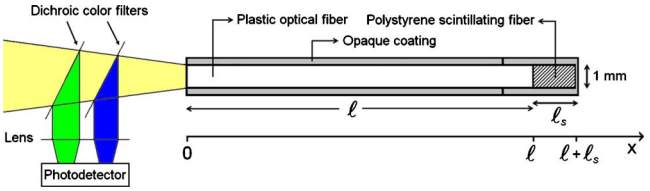

FIG. 1. Typical experimental setup used with the spectral method. The PSD is made of a scintillating fiber of length ℓ_S (usually between 1 and 3 mm) coupled to an optical fiber of length ℓ (between 2 and 20 m). An optical system composed of color filters and a photodetector is used for measuring the light emitted by the PSD in two different spectral regions.

Currently, the state-of-the-art method for the Cerenkov light correction is the one proposed by Fontbonne *et al.*[16] in 2002, which is based on the spectral analysis of the light emitted by PSDs. Figure 1 shows the experimental setup commonly used with this method. The PSD is made of a scintillating fiber of 1 mm diameter and a few millimeters length, coupled to a plastic optical fiber of a few meters length. The setup also includes an optical system composed of color filters and a photodetector for measuring the light emitted by the PSD in two different spectral regions (wavelength intervals). This spectral method has been shown to produce results that agree with reference measurements taken with ionization chambers and no inaccuracies or limitations have been reported in the literature to date. However, most of the published results obtained using this method were measured in situations similar to the calibration conditions where the scintillation light is dominant over the Cerenkov light. To our knowledge, this spectral method has not been tested in situations where the radiation beam is mainly incident on the optical fiber so that the Cerenkov light is the main component of the PSD signal. Such a situation may arise in detector arrays made of PSDs because it is not possible to control which portion of optical fibers will be irradiated in such devices. A Cerenkov light-dominated situation may also arise with a single PSD when measuring the tails of a dose profile with the scintillator located in the low-dose region and the optical fiber located in the high-dose region. We hypothesize that an inaccuracy in the Cerenkov light correction will result in an asymmetric measurement of a symmetrical dose profile depending on the predominance of this contamination light.

The purposes of this work were: (1) To determine if the spectral method could accurately correct the Cerenkov light effect in PSDs in Cerenkov light-dominated situations and (2) to develop a procedural guideline for accurately determining the calibration factors of PSDs. We first demonstrate, using the equations of the spectral method, that the condition for accurately correcting the effect of Cerenkov light is that the ratio of the two calibration factors must be equal to the ratio of the Cerenkov light measured within the two different spectral regions used for analysis. Based on this proof, we propose two new procedures to calibrate PSDs that were designed to respect this condition. The first procedure proposed is characterized by the fact that the determination of the Cerenkov light ratio (CLR) is independent of doses measured with other types of detectors (e.g., ionization chambers and diodes) or calculated by the treatment planning system. The second procedure proposed is particularly suitable for calibrating arrays of PSDs. A PSD that consists of a cylindrical polystyrene scintillating fiber (1.6 mm^3) coupled to a plastic optical fiber was calibrated by using these new procedures and the two reference procedures described in the literature. To validate the extracted calibration factors, relative dose profiles and output factors for a 6 MV photon beam from a medical linac were measured with the PSD and an ionization chamber. Emphasis was placed on situations where the Cerenkov light is dominant over the scintillation light and on situations dissimilar to the calibration conditions.

II. MATERIALS AND METHODS

II.A. The spectral method for Cerenkov light correction in PSDs

II.A.1. Theory

The spectral method for the correction of the Cerenkov light effect in PSDs was first described by Fontbonne *et al.*[16] in 2002 and explicitly formulated by Frelin *et al.*[3] in 2005. This method allows to express the dose deposited in water at the scintillator's location, in absence of the PSD, as a function of the light spectrum emitted by the PSD. We reformulate in this section some aspects of the spectral method to take into account the effect of the optical fiber attenuation on the Cerenkov light spectrum.

Because quenching effects can be neglected at therapeutic energies,[17] the intensity of scintillation light produced in the PSD is proportional to the average dose deposited in the scintillator volume D_S. The number of scintillation photons per unit wavelength injected in the optical fiber at the position $x=\ell$ in Fig. 1 can be expressed as follows:

$$L_S(\lambda) = \eta \cdot q \cdot D_W \cdot S(\lambda), \tag{1}$$

where η is a constant representing the coupling efficiency and the light yield of the scintillator and $S(\lambda)$ is the normalized emission spectrum of the scintillator.[18] The term $q=D_S/D_W$ is the conversion factor between the average dose deposited in the scintillator volume and the dose deposited in water at the scintillator's location in absence of the PSD (D_W). Monte Carlo simulations and/or cavity theory calculations have shown that this conversion factor is close to unity and vary less than 2% for photon energies ranging between 500 keV and 20 MeV.[19,20]

When a PSD is exposed to a megavoltage energy radiation beam, Cerenkov light is also produced in the optical fiber. The intensity of collected Cerenkov light produced at the position x along the PSD axis $[C(x)]$ depends on several unknown parameters including the dose distribution along this axis and the orientation of the beam relative to this axis.[21] Therefore, the production of Cerenkov light is not correlated with the production of scintillation light. Because the emission spectrum of Cerenkov light varies as one over the wavelength squared, the number of Cerenkov photons per unit wavelength collected in the PSD at position x can be expressed as

$$L_C(\lambda,x) = \frac{C(x)}{\lambda^2}. \tag{2}$$

Once emitted, the scintillation and Cerenkov photons are propagated in the optical fiber up to the position $x=0$ in Fig. 1 where they leave the PSD. The emission spectra are modified during this propagation by a factor $A(\lambda,x)=e^{-\phi(\lambda)\cdot x}$, which depends on the attenuation spectrum of the optical fiber $\phi(\lambda)$ and on the location of production x. The number of photons per unit wavelength exiting the PSD can therefore be expressed as

$$L(\lambda) = \eta \cdot q \cdot D_W \cdot S(\lambda) \cdot A(\lambda,\ell) + \lambda^{-2} \cdot \int_0^{\ell} C(x) \cdot A(\lambda,x) \cdot dx, \tag{3}$$

where ℓ is the length of the optical fiber (see Fig. 1). By integrating each side of an equation similar to Eq. (3) on two different spectral regions ($i=1,2$), Frelin *et al.*[3] have shown that the dose deposited in water at the scintillator's location D_W can be expressed as a linear combination of two optical measurements, taken in two different spectral regions within the emission spectra of the PSD. Based on the demonstration by Frelin *et al.*,[3] we define the dose measured by the PSD as

$$D = a \cdot T_1 + b \cdot T_2, \tag{4}$$

where $[a,b]$ are two constants, i.e., the two calibration factors of the PSD and where T_i ($i=1,2$) represents the PSD's light measured in each spectral region. From Eq. (3), the light measured in the spectral region i can be expressed as

$$\begin{aligned} T_i &= \int_0^{\infty} F_i(\lambda) \cdot L(\lambda) \cdot d\lambda \\ &= \eta \cdot q \cdot D_W \int_0^{\infty} F_i(\lambda) \cdot S(\lambda) \cdot A(\lambda,\ell) \cdot d\lambda \\ &\quad + \int_0^{\ell} C(x) \cdot \int_0^{\infty} F_i(\lambda) \cdot \lambda^{-2} \cdot A(\lambda,x) \cdot d\lambda \cdot dx \\ &= \eta \cdot q \cdot D_W \cdot G_i(\ell) + \int_0^{\ell} C(x) \cdot H_i(x) \cdot dx, \end{aligned} \tag{5}$$

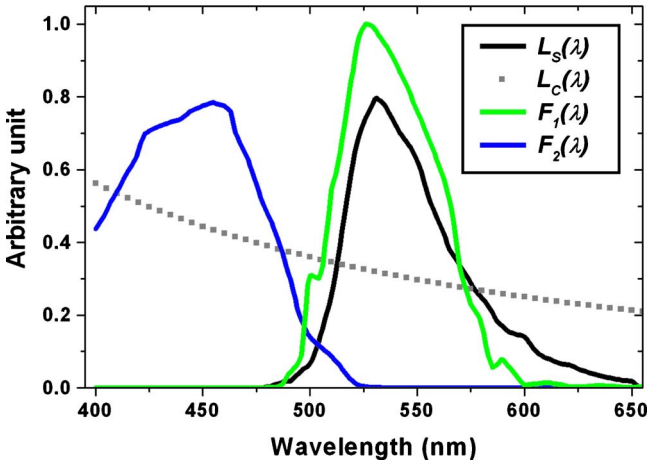

FIG. 2. Emission spectra of scintillation light (BCF-60) and Cerenkov light relative to the two spectral regions used in this work.

where $F_i(\lambda)$ $(i=1,2)$ are the two functions that define the overall optical detection efficiency for the two measurement channels. The spectral dependencies of these functions are mostly determined by the color filters used for the spectral analysis. The terms $G_i(\ell)$ and $H_i(x)$ in Eq. (5) are, respectively, the scintillation spectrum and the Cerenkov spectrum measured within the spectral region i. Figure 2 illustrates the spectral regions used in this work relative to the two emission spectra. By combining Eqs. (4) and (5), the dose measured with the PSD can be expressed as

$$D = \eta \cdot q \cdot D_W \cdot [a \cdot G_1(\ell) + b \cdot G_2(\ell)] + \int_0^{\ell} C(x) \cdot [a \cdot H_1(x) + b \cdot H_2(x)] \cdot dx. \quad (6)$$

We now impose the condition that the dose measured by the PSD must be independent of the Cerenkov light produced in the optical fiber. From Eq. (6), this condition is satisfied in all situations only if $a \cdot H_1(x) + b \cdot H_2(x) = 0$. The ratio of the two calibration factors must therefore be equal to the ratio of Cerenkov light measured within the two spectral regions

$$-\frac{b}{a} = \frac{H_1(x)}{H_2(x)} = \frac{\int_0^{\infty} \lambda^{-2} \cdot F_1(\lambda) \cdot A(\lambda,x) \cdot d\lambda}{\int_0^{\infty} \lambda^{-2} \cdot F_2(\lambda) \cdot A(\lambda,x) \cdot d\lambda}. \quad (7)$$

The relation expressed in Eq. (7) is the necessary condition to accurately correct the effect of Cerenkov light in the PSD. We define the ratio in Eq. (7) as the CLR. By substituting Eq. (7) into Eq. (4), we can express the dose measured by the PSD as

$$D = a \cdot \left[T_1 - \left(\frac{H_1(x)}{H_2(x)} \right) \cdot T_2 \right]. \quad (8)$$

The second condition of the system is that the dose measured must be equal to the dose deposited in water at the scintillator's location: $D = D_W$. According to Eqs. (6) and (7), this condition is realized when

$$a = \frac{1}{\eta \cdot q \cdot G_1(\ell) \cdot \left[1 - \frac{H_1(x)}{H_2(x)} \cdot \frac{G_2(\ell)}{G_1(\ell)} \right]}. \quad (9)$$

The calibration factor a is the gain factor of the PSD. This factor depends on the number of scintillation photons per dose unit measured during the calibration and also on the ratio of Cerenkov light and the ratio of scintillation light, both measured in the two spectral regions.

II.A.2. The condition of validity of the spectral method

We have shown in Sec. II A 1 that the two calibration factors depend on the CLR. However, because of the effect of the optical fiber attenuation, this ratio depends on the location x along the PSD axis where the Cerenkov light is produced. The condition of validity of the spectral method is that the calibration factors must remain constant for all situations encountered during measurements. From Eq. (7), three options are available to maintain the CLR constant. The first option is to choose an optical fiber that has sufficiently low attenuation properties that the attenuation differences between the optical paths of the Cerenkov photons and the optical path of the scintillation photons can be neglected, i.e., $A(\lambda,x) \approx A(\lambda,\ell)$ for all x, where $C(x) \neq 0$. This is the philosophy behind the original formulation of the spectral method. The second option is to choose an optical fiber for which the attenuation is independent of the wavelength of the photons. These two options depend on the characteristics of commercially available plastic optical fibers, a parameter on which users have very little control. However, Eq. (7) points to a third option which is more general. It consists in the optimization of the transmission spectrum $F_i(\lambda)$ of both optical filters to make the following relation true: $\int_0^{\infty} \lambda^{-2} \cdot F_1(\lambda) \cdot A(\lambda,x) \cdot d\lambda = k \cdot \int_0^{\infty} \lambda^{-2} \cdot F_2(\lambda) \cdot A(\lambda,x) \cdot d\lambda$, where k is an arbitrary constant. To our knowledge, this option has never been used in the literature. Therefore, if option 1 or option 2 is not sufficient to generate satisfactory results, the third option could be used to improve the accuracy of the spectral method. However, this option may increase implementation difficulties.

II.B. Characterization of the optical fiber attenuation effect on the CLR

To quantify the impact of the optical fiber attenuation on the CLR, we measured the variation of this ratio as a function of the location x along the optical fiber axis where the Cerenkov light is produced. Measurements were performed on two plastic optical fibers used in recent publications[2,6,15] for their close water equivalence: Eska Premier (Mitsubishi Rayon Co., Ltd., Tokyo, Japan) and BCF-98 (Saint-Gobain Crystals, Paris, France). The Eska Premier optical fiber is made of a PMMA resin core surrounded by a fluorinated polymer cladding (transmission loss $\approx$ 80 dB/km at λ = 500 nm), while the BCF-98 optical fiber is made of a polystyrene core surrounded by a PMMA cladding (transmission

TABLE I. Procedures used to calibrate the PSD. The calibration factors are calculated with Eq. (10) when two calibration doses are required and with Eq. (8) when only one calibration dose is required.

Procedure		Calibration measurements	Calibration dose required
A	A1	Scintillator centered in a 10×10 cm^2 field size	Yes
	A2	Scintillator centered in a 40×40 cm^2 field size with 65 cm of optical fiber irradiated	Yes
B	B1	Scintillator centered in a 10×10 cm^2 field size	Yes
	B2	Scintillator centered in a 40×40 cm^2 field size	Yes
C	C1	Scintillator centered in a 10×10 cm^2 field size	Yes
	C2	Scintillator centered in a 40×40 cm^2 field size	No
	C3	Scintillator centered in a 40×40 cm^2 field size with 65 cm of optical fiber irradiated	No
D	D1	Scintillator centered in a 10×10 cm^2 field size	Yes
	D2	Irradiating a portion of the optical fiber with the scintillator positioned away from the radiation field	Yes[a]

[a]If the scintillator is shielded, this dose could be assumed to be zero.

loss $\approx$ 330 dB/km at $\lambda=500$ nm). A 10 cm length of each optical fiber was irradiated at various locations within 100 cm of the fiber's distal end, i.e., the position $x=\ell$ in Fig. 1. No scintillator was coupled to the optical fibers for these measurements.

II.C. The PSD

The PSD used for dose measurements consisted of a polystyrene scintillating fiber with a diameter of 1 mm and a length of 2 mm (BCF-60, Saint-Gobain Crystals, Paris, France) coupled to a plastic optical fiber (Eska Premier, Mitsubishi Rayon Co., Ltd., Tokyo, Japan) of the same diameter. The emission peak of the scintillator is in the green spectral region $i=1$ ($\lambda_{Peak}=530$ nm). The light of the PSD was separated into two spectral regions using two 45° reflective dichroic color filters (Green NT47–950 and Blue NT47–949, Edmund Optics Inc., Barrington, NJ) and detected with a monochrome charge-coupled device (CCD) camera (Alta U4000, Apogee Instruments Inc., Roseville, CA). Two additional color filters (Green HT738 and Blue HT195, LEE Filters, Hampshire, England) were placed between the CCD camera and their respective dichroic filters. An integration time of 3 s was set on the CCD camera. All measurements were performed in water using a 6 MV photon beam from a Varian Clinac iX linac (Varian Medical Systems, Inc., Palo Alto, CA) and a motorized water tank (Blue Phantom, IBA Dosimetry, Louvain-la-Neuve, Belgium).

II.D. Calibration procedures

We are proposing in this work two new calibration procedures designed to respect the condition expressed by the Eq. (7). We hypothesize that such procedures would guarantee an accurate correction of the Cerenkov light effect. To validate those, we calibrated the PSD by using these two new procedures and the two reference procedures described in the literature. A description of the four procedures used (A, B, C, and D) can be found in Table I.

Procedure A is the one recommended in the paper by Fontbonne *et al.*[16] and in that by Frelin *et al.*[3] It requires performing a measurement for which the optical fiber is rolled in the radiation field to maximize the production of Cerenkov light. In both papers, 1.5 m of optical fiber was irradiated, but according to Fontbonne *et al.*,[16] "the exact length of fiber put in the field is not important. It should just be larger than the greatest length the user will ever need." Procedure B is similar to those used in recent papers, mostly related to arrays of PSDs.[2,6,12] Procedure A is not applicable in these cases because the optical fibers are fixed within phantoms in such devices. Therefore, the production of Cerenkov light is maximized in one of the two calibration measurements by irradiating the PSD with a large field size. To our knowledge, these two calibration procedures have never been compared to each other.

Procedures C and D are the two calibration strategies that we are proposing. For calibration procedure C, the signal difference between measurements C2 and C3 is composed of only Cerenkov light. The CLR can therefore be directly calculated. Care must be taken not to move the scintillator between measurements C2 and C3. In this approach, the calibration factor a was determined by irradiating the PSD with a 10×10 cm^2 field size and using Eq. (8). This procedure has the advantage of being independent of dose measurements taken with other types of detectors (e.g., ionization chambers and diodes) or calculated by the treatment planning system for determining the CLR. Systematic errors related to differences in energy response or dose volume averaging between two types of detectors can therefore be eliminated. For calibration procedure D, we tried to measure the CLR by directly irradiating a length of 15 cm of the optical fiber with the 6 MV photon beam to generate only Cerenkov light in the PSD. However, a small amount of scintillation light produced by the ambient radiation inside the treatment room is added to the Cerenkov light. This scintillation light can be compensated for by either shielding the scintillator or by measuring the dose deposited at the scintillator's location. In this work, the scintillator was positioned 100 cm away from the radiation field and the dose at the scintillator's location was measured with an ionization chamber. This procedure has the advantage of being suitable for

calibrating arrays of PSDs because it maximizes the production of Cerenkov light by simply irradiating the optical fibers at a place located somewhere between the phantom and the optical system.

For all calibration measurements described in Table I except for D2, the scintillator was positioned at the isocenter of the linac at a depth of 10 cm in water. All measurements were repeated 20 times. Calibration doses in water were measured with an IC10 ionization chamber (now CC13, IBA Dosimetry, Louvain-la-Neuve, Belgium) placed at the same location of the scintillator. The IC10 was cross-calibrated in a field 10×10 cm^2 with an A12 ionization chamber (Exradin, Farmer-type, Standard Imaging, Middleton, WI), whose absorbed dose-to-water calibration factor had been determined according to the AAPM's TG-51 protocol.[22] The IC10 is an ionization chamber used for clinical reference dosimetry in the AAPM's TG-51 protocol and in the IAEA's TRS-398 code of practice.[22,23] According to Fraser *et al.*,[24] the variability of the IC10 is less than 0.2% for open fields.

For the procedures that require two calibration doses in Table I, the calibration factors were determined using the following linear system:

$$\begin{bmatrix} a \\ b \end{bmatrix} = \begin{bmatrix} T_1^\alpha & T_2^\alpha \\ T_1^\beta & T_2^\beta \end{bmatrix}^{-1} \cdot \begin{bmatrix} D^\alpha \\ D^\beta \end{bmatrix}, \tag{10}$$

where α and β represent the two calibration events and $[D^\alpha, D^\beta]$ are the calibration doses associated. This is the calculation method commonly used in the literature.[3]

II.E. Validation of the spectral method and of the calibration procedures

To determine which calibration procedures listed in Table I allowed the calibration factors of the PSD to be accurately determined and to determine if the spectral method can accurately correct the Cerenkov light effect, we performed a series of relative dose profile and output factor measurements with the PSD. Emphasis was placed on situations where the Cerenkov light is the dominant component of the PSD's signal because such situations might be especially sensitive to the accuracy of the Cerenkov light correction.

II.E.1. Relative dose profiles

The dose profiles were measured with the PSD in two different configurations. Figure 3(a) shows the symmetric configuration where the PSD was moved by keeping the optical fiber axis perpendicular to the profile axis. This configuration minimizes the production of Cerenkov light by limiting the length of optical fiber irradiated. During the measurement sequence, the variation of the Cerenkov light produced in the PSD was correlated with the variation of the scintillation light and the dose. Figure 3(b) shows the asymmetric configuration, in which the PSD was moved by keeping the optical fiber axis parallel to the profile axis. In this configuration, the amount of Cerenkov light produced in the PSD always increased during the measurement sequence. The PSD signal was dominated by the Cerenkov light in situation 5, shown on Fig. 3(b).

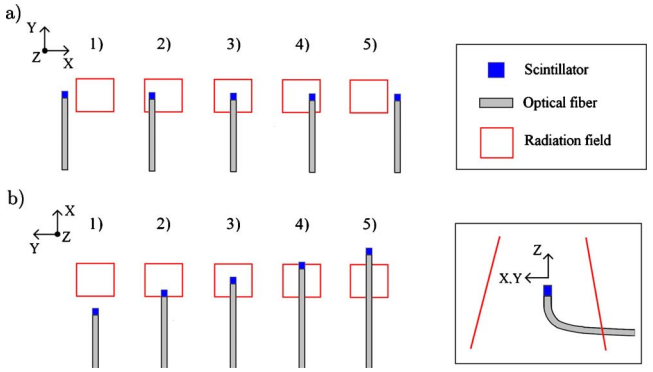

FIG. 3. The two configurations used to measure relative dose profiles along the *X*-axis with the PSD. (a) Symmetric configuration in which the PSD is moved by keeping the optical fiber axis perpendicular to the profile axis during the measurement sequence (from 1 to 5). (b) Asymmetric configuration in which the PSD is moved by keeping the optical fiber axis parallel to the profile axis during the measurement sequence (from 1 to 5). The PSD was mounted vertically along the *Z*-axis in the water tank.

Dose profiles for field sizes of 35×35, 25×25, and 7×7 cm^2 were measured with the PSD in both the symmetric and asymmetric configurations. Dose profiles were also measured with the IC10 ionization chamber. All measurements were performed at a depth of 10 cm in water with a source-to-surface distance (SSD) of 90 cm.

II.E.2. Output factor

Output factors for field sizes ranging from 5×5 to 40×40 cm^2 were measured with the PSD and the IC10 ionization chamber. The measurements were taken in water at the isocenter of the linac (SSD=90 cm, depth=10 cm). Furthermore, to verify that the effect of Cerenkov light produced in the PSD was effectively corrected, we measured the output factor for the 40×40 cm^2 field size in two situations, the first with 30 cm of the optical fiber irradiated and the second with 65 cm of the optical fiber irradiated. The latter case is an extreme condition that does not occur in practice. However, this measurement will help bring out the differences between calibration procedures.

III. RESULTS

III.A. Characterization of the optical fiber attenuation effect on the CLR

Figure 4 shows the variation of the CLR measured as a function of the location of the Cerenkov light production along the optical fiber axis. As shown, the variation of the CLR depends strongly on the type of optical fiber used. For the BCF-98 optical fiber, a variation of more than 12% was observed between the distal end and 75 cm away from the distal end. This variation was limited to 1% for distances up to 100 cm away from the distal end for the Eska Premier optical fiber. For both optical fibers, the Cerenkov light detected when it was produced closer to the photodetector had

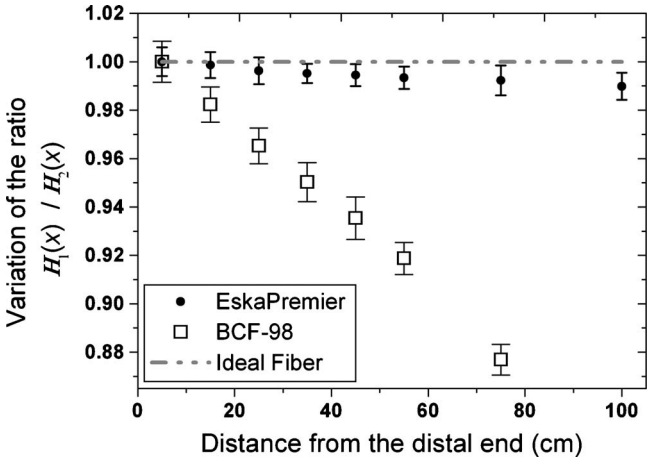

FIG. 4. Variation of the CLR $H_1(x)/H_2(x)$ as a function of the location along the optical fiber axis where the Cerenkov light is produced. Data are normalized to the distal end of the optical fiber. The error bars represent ± 1 standard deviation.

a lower CLR because the attenuation of the optical fibers is higher in the blue spectral region ($i=2$) than in the green spectral region ($i=1$). Based on these results, the PSD used in this work was made with an Eska Premier optical fiber to approaches the ideal situation of a constant CLR, as required by the spectral method.

III.B. Calibration factors of the PSD

Table II presents the calibration factors of the PSD extracted from the four calibration procedures. The calibration factors obtained using calibration procedures A, C, and D were in agreement within 0.22% for the gain factor and 1.8% for the CLR. However, the calibration factors obtained using calibration procedure B differed by more than 1.2% for the gain factor and 11% for the CLR when compared to those from the other calibration procedures. It is particularly interesting to note that the dose values measured with the ionization chamber and used to calculate the calibration factors for procedures A and B are exactly the same (dose at the center of 10×10 and 40×40 cm^2 field sizes); only the amount of Cerenkov light produced between calibration measurements differed between the two procedures. Student's t-tests performed on the CLR distributions showed that the difference between measured values extracted from procedure C and those extracted from procedures A, B, or D was statistically significant ($p<0.000\,01$). The results of dose measurements will allow the determination of which calibration factors listed in Table II are the most accurate.

TABLE II. Calibration factors of the PSD extracted from different calibration procedures. Calibration measurements were repeated 20 times; ± 1 standard error of the mean is used as uncertainty, i.e., standard deviation divided by the square root of the number of measurements

Procedure	Gain factor a	Cerenkov light ratio $-b/a$
A	$1.826\pm0.001\times10^{-6}$	0.507 ± 0.001
B	$1.804\pm0.002\times10^{-6}$	0.454 ± 0.004
C	$1.830\pm0.001\times10^{-6}$	0.516 ± 0.001
D	$1.826\pm0.001\times10^{-6}$	0.507 ± 0.001

III.C. Validation of the spectral method and of the calibration procedures

III.C.1. Dose profiles

Figure 5 presents the dose profiles for field sizes of 35×35, 25×25, and 7×7 cm^2 measured with the PSD in the symmetric and asymmetric configurations. For all field sizes, the relative dose profiles measured in the symmetric configuration were symmetric and agreed with the ionization chamber measurements, regardless of the calibration procedure used. In contrast, the dose profiles measured in the asymmetric configuration were dependent on the calibration procedure used. For field sizes of 35×35 and 25×25 cm^2 [Figs. 5(b) and 5(d), respectively], the calibration factors from procedure B caused the PSD to over-respond in the out-of-field region when the optical fiber was crossing the radiation field and the scintillator was located in the out-of-field region [situation 5 in Fig. 3(b)]. This indicates that the Cerenkov light effect was only partially corrected when using the calibration procedure B. In Figs. 5(b) and 5(d), a clear improvement in the symmetry of the dose profiles was observed when using the calibration factors obtained from procedures A, C, and D. The measured dose profiles were symmetric within 1% of the maximum dose and a more symmetric dose profile was obtained for the 35×35 cm^2 field size than for the 25×25 cm^2 field size.

III.C.2. Output factors

Figure 6 shows the output factors measured with the PSD and the ionization chamber. The data were normalized to a 10×10 cm^2 field size. For each calibration procedure, the PSD response agreed with the ionization chamber at their respective calibration points. Two key observations can be made from Fig. 6. First, the PSD response in the 40×40 cm^2 field size depends on the length of the optical fiber irradiated for calibration procedures A, B, and D, even if the dose at the scintillator's location was the same. This indicates that the Cerenkov light effect was only partially corrected. In contrast, the results obtained using procedure C were not affected by the length of optical fiber irradiated, which indicates an accurate Cerenkov light correction. Second, for all situations, except when 65 cm of optical fiber was irradiated in the 40×40 cm^2 field size, the output factors measured with the PSD by using the calibration factors from procedures A, C, and D produced similar results within uncertainties. The results suggest that PSDs measure output factors that are lower than those measured with the ionization chamber for square field sizes larger than 25×25 cm^2, with a discrepancy of $2.0\pm0.4\%$ for a 40×40 cm^2 field size.

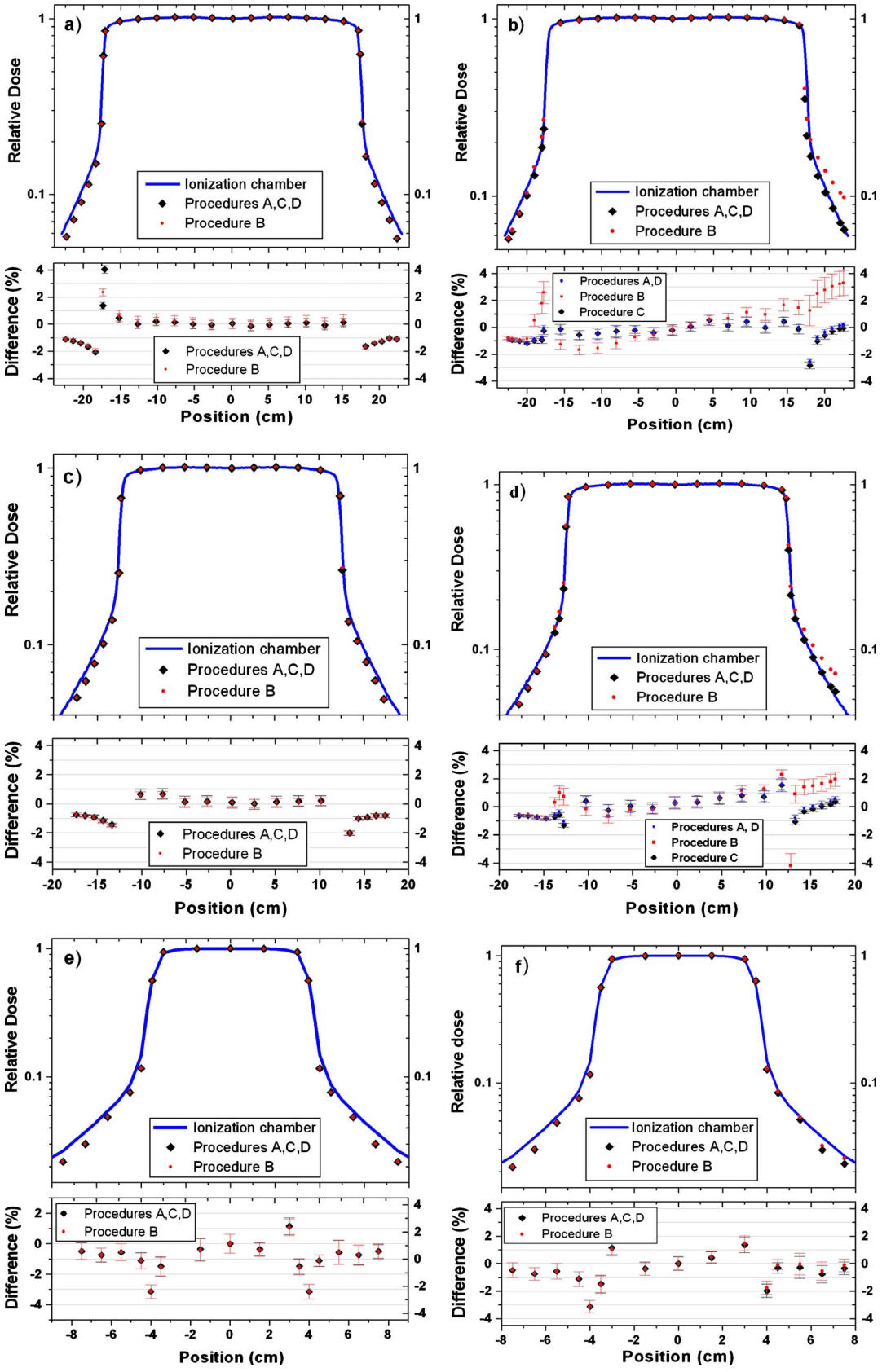

FIG. 5. Relative dose profiles measured in the symmetric configuration (left panels) for field sizes of (a) 35×35, (c) 25×25, and (e) 7×7 cm^2 and differences with the ionization chamber. Relative dose profiles measured in the asymmetric configuration (right panels) for field sizes of (b) 35×35, (d) 25×25, (f) and 7×7 cm^2 and differences with the ionization chamber. Positive positions in (b), (d), and (f) correspond to situations 4 and 5 in Fig. 3(b). To improve the clarity of the figures, the results from different calibration procedures were represented by the same symbol and error bars if the differences between them were not discernible. Error bars represent ±1 standard deviation. Measurements were repeated ten times for the in-field regions and 14 times for the out-of-field regions.

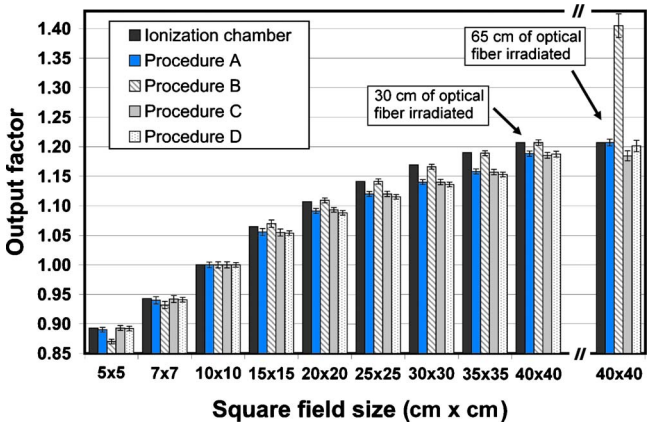

FIG. 6. Output factors measured with the PSD by using the calibration factors extracted from the different calibration procedures and with the ionization chamber. The error bars represent ±1 standard deviation. Measurements were repeated ten times.

III.C.3. The effect of the length of optical fiber irradiated on dose measurements

A summary of the effect of the length of optical fiber irradiated on the measurements of dose profiles and output factors is presented in Table III. In each case, we compared two situations in which the dose at the scintillator's location was the same but the length of optical fiber irradiated was different. For dose profiles, we calculated the difference in dose between two points having the same position in Fig. 5, one from the dose profile taken in the asymmetric configuration and the other from the dose profile taken in the symmetric configuration. The two points were located in the positive part of the position axis in the out-of-field region in Fig. 5. The values presented in Table III are averages for three adjacent positions. We also included in Table III the difference in dose between the output factors of the field size 40×40 cm^2 in Fig. 6, measured with 30 and 65 cm of optical fiber irradiated. Overall, the results show that calibration procedure C produced, on average, the measurements that were the less influenced by the length of optical fiber irradiated and the amount of Cerenkov light produced. This therefore suggests that calibration procedure C has produced the most accurate correction of the Cerenkov light effect. For the two procedures, B and D, that appear suitable for the calibration of arrays of PSDs, the results indicate that procedure D produced the most accurate correction of the Cerenkov light effect.

IV. DISCUSSION

In this work, we examined if the spectral method could accurately correct the Cerenkov light effect in PSDs in various situations including in Cerenkov light-dominated situations. We used four different procedures (A, B, C, and D) to calibrate the PSD and we compared the results to ionization chamber measurements. We found that procedures used for calibrating PSDs have an effect on the calibration factors extracted and, therefore, on the accuracy of dose measurements. Of the four calibration procedures used, Table III has shown that procedure C is the one that has produced the measurements that were the less influenced by the length of optical fiber irradiated and the amount of Cerenkov light produced in the PSD. We can therefore conclude that calibration procedure C has produced the most accurate correction of the Cerenkov light effect. This is not so surprising because this procedure is the only one for which the CLR was directly measured. Among the four calibration procedures, only two of them, B and D, were adapted to the calibration of arrays of PSDs. Results presented in Table III have shown that measurements were less dependent on the amount of Cerenkov light produced when calibration procedure D was used instead of procedure B. A general guideline for the calibration of PSDs can therefore be formulated as follows: When possible, calibration procedures that allow a direct measurement of the CLR, like procedure C in this study, should be used. When such a procedure cannot be applied, our results show that maximizing the difference in the amount of Cerenkov light produced between the calibration measurements reduces the standard deviation of the calibration factors and minimizes the consequences of possible systematic errors associated with the calibration doses.

The results from relative dose profiles show that the spectral method can generate, for various field sizes, symmetrical dose profiles that agree to within 1% with ionization chamber measurements regardless of the configuration (symmetric or asymmetric) in which the measurements are done. This

TABLE III. The effect of additional length of optical fiber irradiated on the dose measurements. For each case, the dose to the scintillator was the same between the two measurements. Dose differences are expressed as percentage of the dose at the center of the field for dose profiles and as percentage of the dose at the center of the field 10×10 cm^2 for the output factor 40×40 cm^2.

Data source	Difference in length of optical fiber irradiated (cm)	Dose difference[a] (%)			
		Procedure A	Procedure B	Procedure C	Procedure D
Dose profile 35×35 cm^2	35	0.6 ± 0.1	3.3 ± 0.3	0.4 ± 0.1	0.6 ± 0.1
Dose profile 25×25 cm^2	25	0.9 ± 0.1	2.3 ± 0.2	0.7 ± 0.1	0.9 ± 0.1
Dose profile 7×7 cm^2	7	0.0 ± 0.4	0.2 ± 0.4	0.0 ± 0.4	0.0 ± 0.4
Output factor 40×40 cm^2	35	1.8 ± 0.2	13.9 ± 0.7	−0.1 ± 0.2	1.5 ± 0.3

[a]±1 standard error of the mean is used as uncertainty.

indicates that the spectral method is a reliable and powerful method for the correction of the Cerenkov light effect in PSDs. However, for measurements taken in the asymmetric configuration, the dose profiles were not perfectly symmetric for larger field sizes (25×25 and 35×35 cm^2), with a more accentuated effect for the 25×25 cm^2 field size. This small amount of asymmetry can be explained by the variation of the CLR shown in Fig. 4. The CLRs extracted from calibration procedures A, C, and D are characteristic of the Cerenkov light produced far from the distal end of the PSD (e.g., between 30 and 65 cm from the distal end for procedure C). This makes the Cerenkov light correction more accurate for situations where the optical fiber is irradiated far from the distal end. For positive positions on Figs. 5(b) and 5(d), this situation is closer to the one encountered in the 35×35 cm^2 field size than in the 25×25 cm^2 field size, making the dose profile more symmetrical. Ultimately, this issue could be resolved by optimizing the spectral regions used for the spectral analysis as discussed in Sec. II A 2. To date, due to the limited choice of commercial plastic optical fibers, we were not able to find an optical fiber that has lower attenuation properties than those of the Eska Premier optical fiber.

Our results suggest that PSDs measure output factors that are lower than those measured with the ionization chamber for square field sizes larger than 25×25 cm^2 with a discrepancy of up to $2.0\pm0.4\%$ for a 40×40 cm^2 field size. Differences in response between the ionization chamber and the PSD were also observed in the out-of-field regions shown in Figs. 5(a), 5(c), and 5(e). At the present time, we cannot determine if the systematic offset between the two types of detectors is caused by an under-response of the PSD or by an over-response of the ionization chamber. Lower energy particles contribute to the dose in larger radiation fields because of the phantom scatter. There is also a strong variation in the energy spectrum in the out-of-field region that depends on the field size and the off-axis distance.[25] Plastic scintillators are known to have reduced scintillation efficiency to electrons with a very low energy (<125 keV) due to quenching effects.[17] Frelin *et al.*[26] studied the linearity of various plastic scintillators and reported their linearity to electrons above 100 keV and to photons above 200–250 keV. In contrast, the response of ionization chambers depends strongly on the energy spectrum and can be affected by the irradiation of the stem of the chamber. Some studies have reported discrepancies between Monte Carlo simulations and ionization chamber measurements for output factors in large radiation fields. For instance, Ding[27] recently compared Monte Carlo simulations (using EGSnrc user code BEAMnrc) to ionization chamber measurements for output factors using a 6 MV photon beam from a Varian CL2100EX linac. The measurements were performed with an IC10 in conditions similar to those used in this work: Water phantom ($48\times48\times48$ cm^3) at a depth of 10 cm with a source-detector distance of 100 cm. The Monte Carlo simulations predicted an output factor (normalized to 10×10 cm^2) that was 1.3% lower than the output factor measured with the IC10 for a square field size of 40×40 cm^2. Although the statistical uncertainty of the Monte Carlo calculations was about 1%, Ding's results exhibit the same trend as the PSD measurements presented in Fig. 6. Furthermore, Fippel *et al.*[28] performed a full Monte Carlo simulation (using EGSnrc user code BEAMnrc) of the head of an Elekta SL*i* Plus accelerator. They compared the predicted output factors for a 6 MV photon beam at a depth of 10 cm in water for field sizes of 30×30 and 40×40 cm^2 to those measured with an ionization chamber and found that they were lower ($\sim2\%$). More investigations need to be performed before formulating a stronger statement on this issue.

We focused in this work on measurements taken in Cerenkov light-dominated situations and with large field sizes ($>20\times20$ cm^2) because more Cerenkov light has to be removed for these cases. However, promising applications of PSDs is their use for dosimetry in intensity-modulated radiation therapy and radiosurgery which are characterized by much smaller radiation fields. The present study constitutes, therefore, a stringent validation of the spectral method and indicates that this method is highly reliable. However, we found that it is difficult to accurately determine the calibration factors without maximizing the difference in the amount of Cerenkov light produced between the calibration measurements, which means that portions of the optical fiber far from the distal end have to be irradiated. The extracted calibration factors are therefore affected by the attenuation of the optical fiber as shown in Fig. 4.

V. CONCLUSION

In this work, we determined that the spectral method can be used to accurately correct the Cerenkov light effect in PSDs. We found that the accuracy of the spectral method depends on the calibration procedure used to determine the calibration factors of the PSD and on the attenuation properties of the optical fiber used. Results from the relative dose profiles measurements showed that this method can correct the Cerenkov light effect with an accuracy level of 1%. Collectively, our results suggest that PSDs measure output factors that are lower than those measured by ionization chambers for square field sizes larger than 25×25 cm^2, which is consistent with previously published Monte Carlo results. In conclusion, the spectral method is a reliable and powerful method for the correction of the Cerenkov light effect in PSDs.

ACKNOWLEDGMENTS

This work was supported by grants from the Natural Sciences and Engineering Research Council (NSERC) (Discovery Grant No. 262105) and the National Cancer Institute (NCI) (Grant No. CA120198-01A2). Mathieu Guillot is financially supported by a NSERC postgraduate scholarship.

[a]Author to whom correspondence should be addressed. Electronic mail: abeddar@mdanderson.org; Telephone: (713) 563-2609; Fax: (713) 563-2479.

[1]R. Alfonso, P. Andreo, R. Capote, M. S. Huq, W. Kilby, P. Kjäll, T. R. Mackie, H. Palmans, K. Rosser, J. Seuntjens, W. Ullrich, and S. Vatnitsky, "A new formalism for reference dosimetry of small and nonstand-

ard fields," Med. Phys. **35**, 5179–5186 (2008).
[2]L. Archambault, A. S. Beddar, L. Gingras, F. Lacroix, R. Roy, and L. Beaulieu, "Water-equivalent dosimeter array for small-field external beam radiotherapy," Med. Phys. **34**, 1583–1592 (2007).
[3]A.-M. Frelin, J.-M. Fontbonne, G. Ban, J. Colin, M. Labalme, A. Batalla, A. Isambert, A. Vela, and T. Leroux, "Spectral discrimination of Cerenkov radiation in scintillating dosimeters," Med. Phys. **32**, 3000–3006 (2005).
[4]J. Lambert, D. R. McKenzie, S. Law, J. Elsey, and N. Suchowerska, "A plastic scintillation dosimeter for high dose rate brachytherapy," Phys. Med. Biol. **51**, 5505–5516 (2006).
[5]S. Beddar, L. Archambault, N. Sahoo, F. Poenisch, G. T. Chen, M. T. Gillin, and R. Mohan, "Exploration of potential of liquid scintillators for real-time 3D dosimetry of intensity modulated proton beams," Med. Phys. **36**, 1736–1743 (2009).
[6]F. Lacroix, L. Archambault, L. Gingras, M. Guillot, A. S. Beddar, and L. Beaulieu, "Clinical prototype of a plastic water-equivalent scintillating fiber dosimeter for QA applications," Med. Phys. **35**, 3682–3690 (2008).
[7]A. S. Beddar, T. R. Mackie, and F. H. Attix, "Water-equivalent plastic scintillation detectors for high-energy beam dosimetry: II. Properties and measurements," Phys. Med. Biol. **37**, 1901–1913 (1992).
[8]V. Collomb-Patton, P. Boher, T. Leroux, J.-M. Fontbonne, A. Vela, and A. Batalla, "The DOSIMAP, a high spatial resolution tissue equivalent 2D dosimeter for LINAC QA and IMRT verification," Med. Phys. **36**, 317–328 (2009).
[9]A. S. Beddar, T. R. Mackie, and F. H. Attix, "Cerenkov light generated in optical fibres and other light pipes irradiated by electron beams," Phys. Med. Biol. **37**, 925–935 (1992).
[10]J. D. Jackson, *Classical Electrodynamics*, 3rd ed. (Wiley, New York, 1998).
[11]A. S. Beddar, T. R. Mackie, and F. H. Attix, "Water-equivalent plastic scintillation detectors for high-energy beam dosimetry: I. Physical characteristics and theoretical considerations," Phys. Med. Biol. **37**, 1883–1900 (1992).
[12]L. Archambault, A. S. Beddar, L. Gingras, R. Roy, and L. Beaulieu, "Measurement accuracy and Cerenkov removal for high performance, high spatial resolution scintillation dosimetry," Med. Phys. **33**, 128–135 (2006).
[13]J. Lambert, Y. Yin, D. R. McKenzie, S. Law, and N. Suchowerska, "Cerenkov-free scintillation dosimetry in external beam radiotherapy with an air core light guide," Phys. Med. Biol. **53**, 3071–3080 (2008).
[14]J. Lambert, Y. Yin, D. R. McKenzie, S. H. Law, A. Ralston, and N. Suchowerska, "A prototype scintillation dosimeter customized for small and dynamic megavoltage radiation fields," Phys. Med. Biol. **55**, 1115–1126 (2010).
[15]F. Lacroix, M. Guillot, M. McEwen, C. Cojocaru, L. Gingras, S. Beddar, and L. Beaulieu, "Extraction of depth dependent perturbation factors for parallel-plate chambers in electron beams using a plastic scintillation detector," Med. Phys. **37**, 4331–4342 (2010).
[16]J. M. Fontbonne, G. Iltis, G. Ban, A. Battala, J. C. Vernhes, J. Tillier, N. Bellaize, C. Le Brun, B. Tamain, K. Mercier, and J. C. Motin, "Scintillating fiber dosimeter for radiation therapy accelerator," IEEE Trans. Nucl. Sci. **49**, 2223–2227 (2002).
[17]G. F. Knoll, *Radiation Detection and Measurement*, 3rd ed. (Wiley, New York, 1989).
[18]A. S. Beddar, S. Law, N. Suchowerska, and T. R. Mackie, "Plastic scintillation dosimetry: Optimization of light collection efficiency," Phys. Med. Biol. **48**, 1141–1152 (2003).
[19]M. A. Clift, R. A. Sutton, and D. V. Webb, "Water equivalence of plastic organic scintillators in megavoltage radiotherapy bremsstrahlung beams," Phys. Med. Biol. **45**, 1885–1895 (2000).
[20]A. S. Beddar, T. M. Briere, F. A. Mourtada, O. N. Vassiliev, H. H. Liu, and R. Mohan, "Monte Carlo calculations of the absorbed dose and energy dependence of plastic scintillators," Med. Phys. **32**, 1265–1269 (2005).
[21]A. S. Beddar, N. Suchowerska, and S. H. Law, "Plastic scintillation dosimetry for radiation therapy: Minimizing capture of Cerenkov radiation noise," Phys. Med. Biol. **49**, 783–790 (2004).
[22]P. R. Almond, P. J. Biggs, B. M. Coursey, W. F. Hanson, M. S. Huq, R. Nath, and D. W. O. Rogers, "AAPM's TG-51 protocol for clinical reference dosimetry of high-energy photon and electron beams," Med. Phys. **26**, 1847–1870 (1999).
[23]P. Andreo, D. T. Burns, K. Hohlfeld, M. S. Hu, T. Kanai, F. Laitano, V. G. Smyth, and S. Vynckier, "Absorbed dose determination in external beam radiotherapy: An international code of practice for dosimetry based on standards of absorbed dose to water," IAEA Technical Reports Series No. 398 (International Atomic Energy Agency, Vienna, 2000).
[24]D. Fraser, W. Parker, and J. Seuntjens, "Characterization of cylindrical ionization chambers for patient specific IMRT QA," J. Appl. Clin. Med. Phys. **10**, 241–251 (2009).
[25]G. X. Ding, "Energy spectra, angular spread, fluence profiles and dose distributions of 6 and 18 MV photon beams: Results of Monte Carlo simulations for a Varian 2100EX accelerator," Phys. Med. Biol. **47**, 1025–1046 (2002).
[26]A.-M. Frelin, J.-M. Fontbonne, G. Ban, J. Colin, and M. Labalme, "Comparative study of plastic scintillators for dosimetric applications," IEEE Trans. Nucl. Sci. **55**, 2749–2756 (2008).
[27]G. X. Ding, "Using Monte Carlo simulations to commission photon beam output factors—A feasibility study," Phys. Med. Biol. **48**, 3865–3874 (2003).
[28]M. Fippel, F. Haryanto, O. Dohm, F. Nüsslin, and S. Kriesen, "A virtual photon energy fluence model for Monte Carlo dose calculation," Med. Phys. **30**, 301–311 (2003).